PROCEEDINGS of the
23rd International Congress on Acoustics

9 to 13 September 2019 in Aachen, Germany

Increased Radiation Efficiency Using Band Gap Effect

Jaesoon JUNG[1]; Cheol-Ho JEONG[1]; Jakob S. JENSEN[2]

[1] Department of Electrical Engineering, Technical University of Denmark, Denmark

[2] Department of Mechanical Engineering, Technical University of Denmark, Denmark

ABSTRACT

Periodic arrangements of elements, such as scatterers, local resonators, and inertial amplifications can induce band gap phenomena, which result in vibration isolation in mechanical systems due to a significant reduction in the energy transmission from source to receiver. This effect has led to vibro-acoustic applications focusing mainly on the reduction of structure-borne noise. Here, we propose to broaden the application range by utilizing the band gap effect to increase the efficiency of sound radiation from vibrating mechanical structures. The increase in radiation efficiency is caused by the enhanced vibration localization near the excitation point. In order to illustrate the phenomenon, a one-dimensional mass-spring model with periodically placed local resonators is examined and with this theoretical model vibration localization and sound radiation efficiency are analyzed.

Keywords: Band gap, Sound radiation, Radiation efficiency, Plate

1. INTRODUCTION

Passive control of vibro-acoustic response by utilizing novel materials has long been an interesting subject of research. As a promising candidate, the metamaterials based on the band gap phenomenon, which is realized by periodically arranging local resonators, has received great attention recently [1-3]. Liu et al. demonstrated that the band gap-based metamaterial can reduce the structure-borne noise transmission significantly. This metamaterial was fabricated with a periodic resonator composed of a lead ball and a silicone rubber coating [1]. After this pioneering work, the band gap has led to many vibro-acoustic applications focusing mainly on the reduction of structure-borne noise [2,3]. For these applications, it is generally regarded that the reduction of vibration results in the reduction of noise. However, the efficiency of sound radiation has received less attention, although it plays an important role in the interaction between vibration and sound. Furthermore, in a previous study, it was found that the efficiency of sound radiation may increase and may thus neutralize the benefit of band gap for noise reduction [4].

Based on the increased radiation efficiency, in this work, we propose a way to broaden the application range by utilizing the band gap to enhance sound radiation. The key idea of this approach is confining vibrations at a localized zone using the band gap. Fig. 1 describes the problem in which resonators bound the sound radiation zone with spatial periodicity of a. To illustrate this idea, a theoretical model based on a thin plate with periodically placed single degree of freedom resonators is developed in Section 2. Using the theoretical model, characteristics of vibration and sound radiation are examined in Section 3. To support the theoretical study, an experimental validation is carried out in Section4. Finally, Section 5 concludes this work.

[1] jjung@elektro.dtu.dk

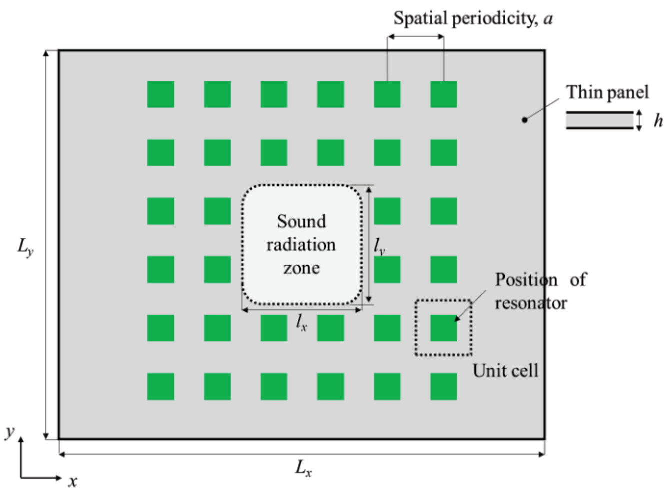

Figure 1 Description of the problem

2. THEORETICAL BACKGROUND

2.1 Structure modelling

We consider a periodic unit cell structure, which is composed of a thin plate and a mass-spring resonator as described in Fig. 2(a). Assuming a harmonic motion, free vibration of the plate can be described with thin plate theory as,

$$-\omega^2 \rho w + D\nabla^4 w = 0, \tag{1}$$

where ω is the angular frequency, w is the vertical displacement, ∇^4 is the biharmonic operator, ρ is the mass density, and D is the bending rigidity ($D = Eh^3/12(1\text{-}v)$) which is expressed with the elastic modulus E, the thickness h, and the Poisson's ratio v. Furthermore, the equation of motion of the mass-spring resonator can be expressed as,

$$-\omega^2 m_r w_r + k_r \left(w_r - w_p\right) = 0, \tag{2}$$

where m_r and k_r are the mass and stiffness of the resonator, w_r and w_p are dofs of the resonator and the plate at the connection point. Employing the finite element method, Eq. (1) can be discretized and combined with Eq. (2) as a matrix equation as,

$$\left(-\omega^2 \mathbf{M} + \mathbf{K}\right)\mathbf{w} = \mathbf{0}, \tag{3}$$

where **M**, **K** are the mass and stiffness matrices, and **w** is the displacement vector.

With the assumption that the unit cell structure is infinitely periodic, wave functions propagating in the band gap structure follow the Bloch theorem [3], which is stated as,

$$\mathbf{w}\left(\mathbf{r}+\mathbf{a}\right) = \mathbf{w}\left(\mathbf{r}\right)e^{j\mathbf{ka}}, \tag{4}$$

where **r** is a position vector inside a unit cell, **a** is the lattice vector ($\mathbf{a} = (a_x, a_y)$), and **k** is the bending wave vector ($\mathbf{k} = (k_x, k_y)$). The term $e^{j\mathbf{ka}}$ represents the amplitude and phase change, which is determined by the wave vector **k** and lattice vector the **a**.

Combining Eq. (3) and Eq. (4), a dispersion equation which defines the relation between wave vector **k** and frequency ω can be obtained as [2,3],

$$\left(-\omega^2 \tilde{\mathbf{M}}\left(\mathbf{k}\right) + \tilde{\mathbf{K}}\left(\mathbf{k}\right)\right)\mathbf{w} = \mathbf{0}, \tag{5}$$

where the tilde symbol represents the modification of matrices.

To obtain a dispersion relation for the band gap structure, Eq. (5) needs to be solved for every possible combinations of wave vectors, but due to symmetry, we may confine the wave vectors to the irreducible Brillouin zone (IBZ) which is described in Fig. 2(b). Usually the wave vectors are further reduced to the boundary of the IBZ, (i.e., Γ→X, X→M, and M→ Γ) because the dispersion curve obtained by solving Eq. (5) along the contour contains sufficient information to identify band gaps.

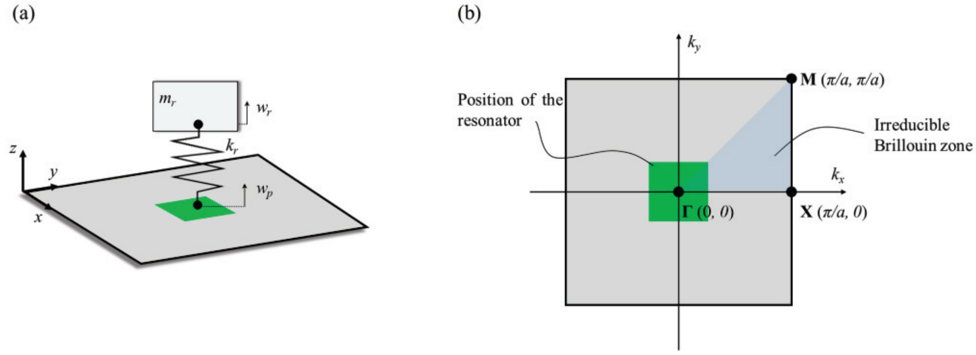

Figure 2 Unit cell structure (a) and wave vector space (b)

2.2 Sound radiation modelling

The sound pressure p, which is radiated from a baffled and flat plate can be calculated based on the Rayleigh integral as [5],

$$p = \frac{j\omega\rho_0}{2\pi}\int_S \frac{ve^{-jkR}}{R(\mathbf{r},\mathbf{r}_0)}dS, \tag{6}$$

where ρ_0 is the mass density of air (1.2 kg/m^3), k is the wave number of acoustic wave ($=\omega/c_0$, c_0 = 343 m/s), R is the distance between the field point $\mathbf{r}_0$ and the surface point $\mathbf{r}$, v is the surface normal velocity, and S is the surface area. Here, the plate is considered stiff enough to neglect the air loading.

Using Eq. (6) the radiation efficiency [5] which is dimensionless quantity measuring the efficiency of sound radiation can be calculated as,

$$\sigma = \frac{\Pi}{\rho_0 c_0 \int_S vv^* dS}, \tag{7}$$

$$\Pi = \int_S \mathrm{Re}\left\{\frac{pv^*}{2}\right\} dS, \tag{8}$$

where Π is the sound power and the asterisk denotes the complex conjugate.

3. SIMULATION RESULTS

3.1 Simulation conditions

Using the theoretical model, simulations are performed to examine the vibration and sound radiation features of the band gap structure. A thin acrylic plate with dimensions of 800 mm × 600 mm × 3 mm is considered. The material properties of the acrylic are elastic modulus of 3.1 GPa, Poisson's ratio of 0.38, mass density of 1165 kg/m^3, and a loss factor of 0.2. To create a band gap, 768 resonators are periodically distributed on the plate with the periodicity of 25 mm. The resonator parameters (i.e., m_r = 5.2 g, k_r = 18.47 kN/m) are determined to adjust band gap at the frequency range of interest (i.e., 300-500 Hz). Every edges of the plate are clamped and a surface force of 1 N/m^2 is applied at the center. Finally, a square sound radiation zone is created at the center of the plate by removing resonators.

3.2 Band gap property

The propagation of bending waves is analyzed with the dispersion curve which describe the relation between frequency and wave vector. Using Eq. (5), the dispersion curve is obtained as shown in Fig.

3(a). In this figure, the band gap, which mismatches with wave vectors, is identified ranging from 300 Hz to 549 Hz. At the upper bound of the band gap, i.e., 559 Hz, the flexural wave dispersion coincides with the acoustic wave dispersion since the periodic resonators slow down the speed of propagation of flexural waves. Around this frequency, sound radiates effectively due to the matching between acoustic wavelength and flexural wavelength, which is known as the coincidence effect.

In the finite periodic structure, the band gap can be analyzed with eigen frequency distribution as shown in Fig. 3(b). In contrast to the distributed eigenfrequency spectrum of the bare structure, the band gap structures have separated eigenfrequency spectra. The fully filled band gap structure has no eigenfrequencies in the band gap range where no standing waves are formed. When the square zone is created by removing resonators, several discretely located eigenfrequencies intrude the empty band. These are localized modes. The small zone with 50 mm edge length has a single localized mode at 487 Hz whereas the larger zone with 100 mm edge length has double localized modes at 348 Hz and 506 Hz. The formation of the localized modes is determined by the parameters of the zone for example, dimensions, material properties, and shape.

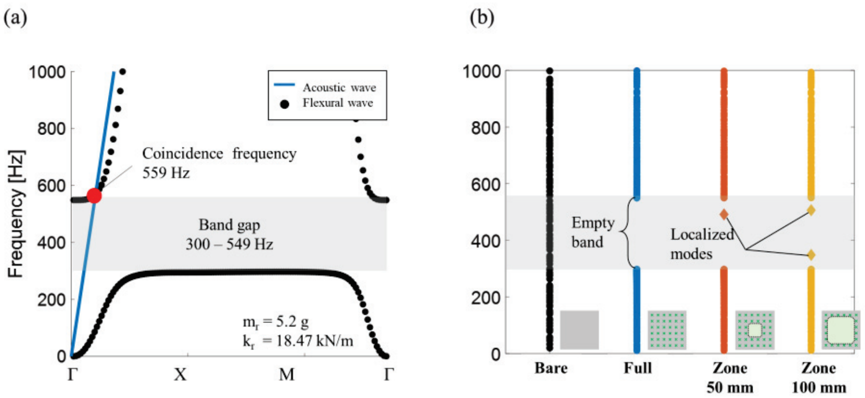

Figure 3 Dispersion curve (a) and eigenfrequency distributions (b)

Fig 4(a) displays the mode shapes of the larger zone with 100 mm edge length. For an ordinary plate structure, as the order of the mode increases mode shapes become distributed and complicated. However, the localized modes are simple and advantageous for sound radiation due to the small cancellation between acoustic waves in the near field. To verify this concept, modal radiation efficiencies, which is calculated using the mode shape vectors and Eq. (7) is presented in Fig. 4(b).

The localized modes B and C show logarithmically increasing radiation efficiency at the frequency range from 100 to 1000 Hz. This smooth behavior attribute to the small interference of acoustic waves due to the simple mode shapes. On the other hand, the distributed mode shapes at A and D show fluctuating radiation efficiencies caused by a large interference of acoustic waves. For frequencies below 500 Hz, the localized mode B outperforms other modes with highly increased radiation efficiency. Thus, the localized mode can be used to enhance sound radiation at the frequency of interest ranging from 300 to 500 Hz.

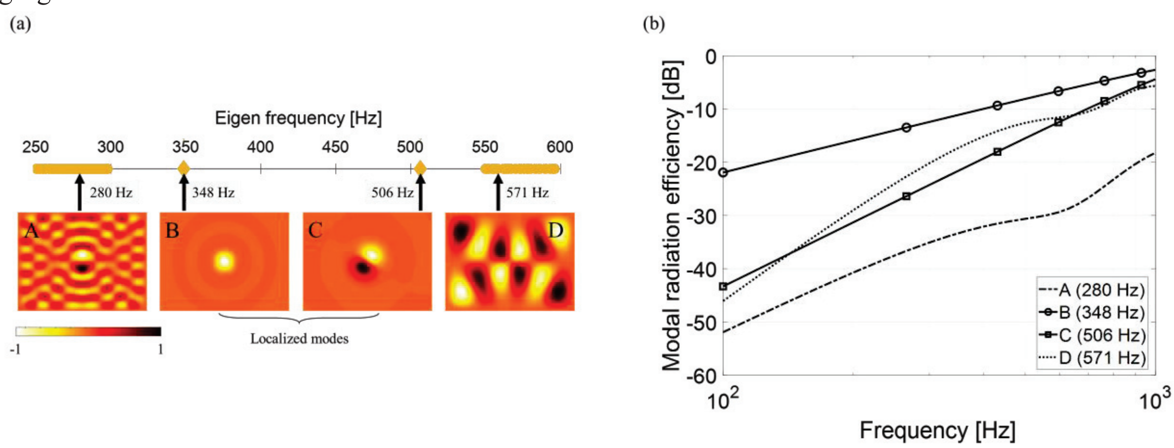

Figure 4 Mode shapes of the 100 mm zone (a) and modal radiation efficiency (b)

3.3 Sound radiation

To analyze the sound radiation of the band gap structure, sound pressure levels (SPLs) 1 m away from the center of the plate are calculated using Eq. (6). Fig. 5 displays SPLs for four different cases. For small zones (Full and 50 mm), the SPLs are significantly reduced but gradually increase within the band gap. On the other hand, for the larger zone with 100 mm edge length, the SPL increases over the bare structure within the band gap frequency. For this case, the SPL peak appears at 348 Hz which corresponds to the frequency of localized modes. The smooth SPL response is obtained due to the small number of peaks.

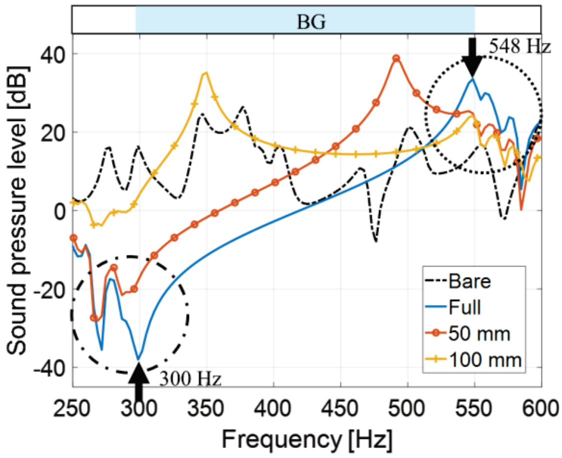

Figure 5 Sound pressure levels for different cases

At the lower bound of the band gap (300 Hz), dips appear for the cases of small zones (full and the 50 mm). These dips can be interpreted with the cancellation of acoustic waves on the surface due to the out of phase vibration induced by the resonator. Fig. 6(a) illustrates the cancellation by describing the vibration velocity field of the full band gap structure at 300 Hz. These cancellation effects are alleviated for the large zone (100 mm) where the out of phase vibration is distant from the center.

At the upper bound of the band gap (548 Hz), common peaks appear for band gap structures. These peaks match with the coincidence between acoustic and flexural waves as shown in Fig. 3(a). The uniform vibration velocity field displayed in Fig. 4(b) supports the occurrence of coincidence effect at the upper bound of the band gap.

The radiation efficiencies of band gap structures are displayed in Fig. 7. The peaks and dips of the radiation efficiency at the upper and lower bounds of the band gap are observed. For the large zone, the radiation efficiency increases by 10 dB above 400 Hz in comparison with the bare structure.

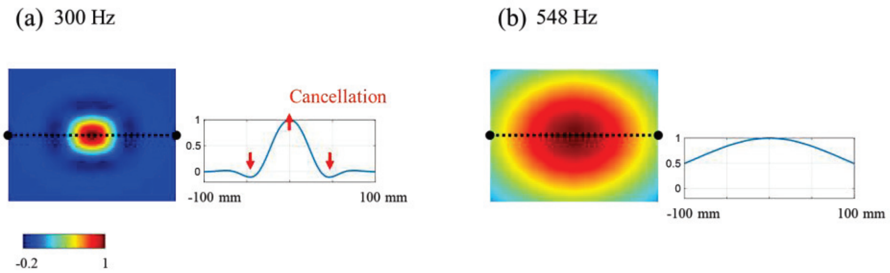

Figure 6 Vibration velocity field at the dip frequency (a) and peak frequency (b)

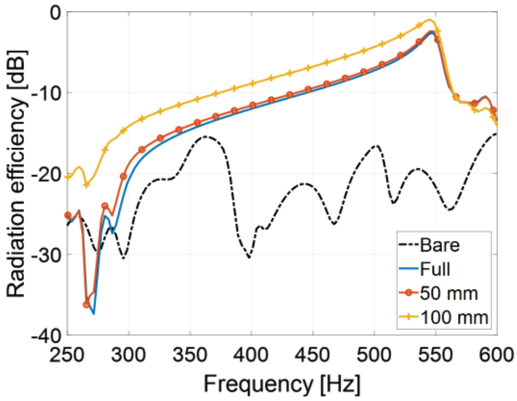

Figure 7 Radiation efficiency

4. CONCLUSIONS

In this work, we have demonstrated the increased efficiency of sound radiation using a band gap structure. A theoretical model is developed based on the thin plate theory and the Bloch theorem. Mass-spring resonators are periodically arranged on the plate to create the band gap ranging from 300 to 549 Hz. The sound radiation from the vibrating band gap structure is modelled using the Rayleigh integral formulation. From simulations, we found that the band gap structures localize vibration at a certain zone and the localized vibrations amplify the sound pressures with small number of resonances. These effects lead to the smoothed frequency response and the increased efficiency of sound radiation.

ACKNOWLEDGEMENTS

This work was supported by the Technical University of Denmark (Signature project).

REFERENCES

1. Z. Liu, X. Zhang, Y. Mao, Y. Y. Zhu, Z. Yang, C. T. Chan, and P. Sheng, Locally Resonant Sonic Materials. Science 2000; 289(5485), 1734
2. C. Claeys, E. Deckers, B. Pluymers, and W. Desmet, A lightweight vibro-acoustic metamaterial demonstrator: Numerical and experimental investigation. Mech. Syst. Signal Process. 2016; 70: 753-880
3. J. Jung, H.-G. Kim, S. Goo, K.-J. Chang, and S. Wang, Realisation of a locally resonant metamaterial on the automobile panel structure to reduce noise radiation. Mech. Syst. Signal Process. 2019; 122: 206-231
4. C. Claeys, P. Sas, W. Desmet, On the radiation efficiency of local resonance based stop band materials. J Sound Vib. 2014; 333(14): 3203-3213
5. S. J. Elliot and M. E. Johnson, Radiation modes and the active control of sound power. J Acoust Soc Am. 1993; 94.4: 2194-2204